Parametric Study to Correlate the Applied Factors and Abrasive Wear Resistance of HVOF Coating

Satpal Sharma

(Submitted October 6, 2011; in revised form April 3, 2012)

Co-Ni-base powder was modified with the addition of CeO_2 to study the effect of CeO_2 addition on microstructure, hardness, and abrasive wear behavior of the unmodified (without CeO_2) and modified (with CeO_2) HVOF sprayed coatings. To investigate the abrasive wear behavior of coatings statistical response surface methodology (RSM) with four factors such as load, abrasive size, sliding distance, and temperature with three levels of each factor were used. Analysis of variance (ANOVA) was carried out to determine the significant factors and their interactions. Thus abrasive wear model was developed in terms of main factors and their significant interactions. The validity of the model was evaluated by conducting experiments under different wear conditions. A comparison of modeled and experimental results showed 2-8% error. The wear resistance of coatings increased with the addition of CeO_2. This is due to increase in hardness with the addition of CeO_2 in Co-Ni-base coatings.

1. Introduction

Thermal spray processes are being widely used due to their relatively high deposition rates and capability of depositing all materials that have a liquid phase. Therefore, many researchers have been using different processes and various types of materials and their modifications for spraying. Among many of the advanced spray technologies, high velocity oxy-fuel (HVOF) is considered to be one of the most widely used techniques (Ref 1). Some engineering applications of HVOF coating technology include the power generation (low temperature super heater), cement industry (fan blades), chemical and petrol industry, earth moving, agriculture and mining, food and sugar industry, forging, glass, pulp and paper, textile, steel making/metal forming, etc., for depositing wear, corrosion and oxidation resistance coatings (Ref 2).

The coating materials are basically classified as Co-, Ni-, and Fe-based. Each of type is commonly used for different specific applications. Hardness of the deposited materials plays an important role in abrasive wear resistance of materials (Ref 3). Besides hardness, other factors which influence abrasive wear have been described in section 2.2. In some cases, hardness can be used as a criterion for comparing abrasive resistance of materials. However, it was also reported that the abrasive resistance can vary for different types of coating materials, even for materials with very similar hardness (Ref 4).

A number of researchers (Ref 5-10) have studied the coatings with varying amount of WC, CrC, and TiC in Co-base alloys. Increase in hardness of Co-base alloys with the addition of WC and TiC has been reported (Ref 11, 12). Maiti et al. (Ref 13) reported that with addition of WC up to 20% in WC-Co-Cr coatings increases the hardness and abrasive wear résistance and further addition of WC increases hardness marginally.

The refining and purifying effects (Ref 14-20), excellent tribological properties (Ref 15, 17, 18, 20), increased corrosion resistance (Ref 14, 16) as well as, mechanical properties (Ref 15) and oxidation resistance of CeO_2 modified Ni- and Fe-based alloy coatings prepared by various processes have been reported (Ref 14-20). Rare earth elements have been widely used in Ni-base alloy coatings (Ref 14-22) but according to the knowledge of author a very little literature was published on Co-Ni-base coatings modified with CeO_2 or La_2O_3 (Ref 23, 24). Hence in the present work, microstructure, hardness, and wear resistance of the Co-Ni-based coatings modified with rare earth elements was investigated using response surface methodology (RSM) in order to understand the individual and combined effect of applied factors on abrasive wear resistance of coatings.

2. Experimental Procedure

2.1 Materials, Methods, and Characterization of Coatings

The carbon steel substrate of SA210GrA1 grade having nominal composition of 0.3%C, 0.6%Mn, 0.29%Si, Bal-Fe (wt.%) was used. The preparation of the substrate before

Satpal Sharma, Gautam Buddha University, Greater Noida 201310, UP India. Contact e-mail: satpal78sharma@gmail.com.

coating deposition was described elsewhere (Ref 25). The nominal composition of used EWAC 1006EE powder was 3.25%C, 29%Cr, 0.6%Mn, 0.35%Si, 5.5%W, 22.5%Ni Bal-Co (wt.%). The average particle size of the used powder was $-90+15\ \mu m$ and its morphology is shown in Fig. 1. This powder was modified by adding 0.8wt.%CeO_2. In further discussions, the EWAC 1006EE powder without CeO_2 and with 0.8wt.%CeO_2 were designated as unmodified 1006 and modified 1006C powders/coatings, respectively. The coating characterizations methods were described elsewhere (Ref 21, 22, 25). The main parameters of HVOF process are shown in Table 1. The substrate was preheated to $200 \pm 10\ °C$ by HVOF flame itself so as to get the uniform temperature of the substrate, afterwards coating deposition was started. The HVOF process was automatic and robotic controlled.

2.2 Factorial Design of Experiment

In the literature, the vast amounts of wear data have been generated by varying one factor at a time approach of experiments. This is the main reason why load has always been considered first in wear research, whilst other factors, e.g., abrasive grain size, sliding distance, temperature, and their combined effects (load and abrasive size, load and speed, abrasive size, and sliding distance), which may also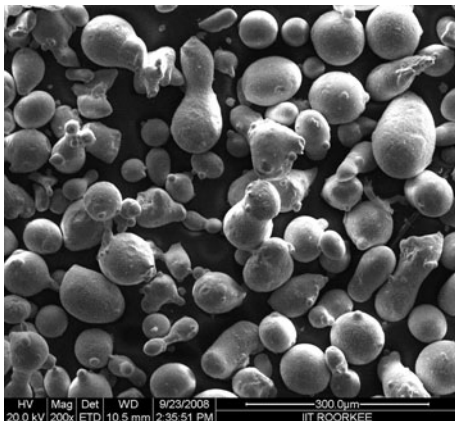 be important, have not been given the attention they deserve. In one factor at a time approach; it is difficult to evaluate the combined (interaction) effects of applied factors, which can be conveniently studied by design of experiment (DOE) and response surface methodology (RSM). The advantage of the statistical method is thus obvious (Ref 26).

The abrasive wear is influenced by a number of different factors such as the properties of the materials (microstructure and hardness), the service conditions (applied load and abrasive grit size), and environment (temperature and humidity). According to Rabinowicz's classic theory (Ref 27) that claims applied load and hardness (depends upon composition) of materials are the most important factors affecting the abrasion process, therefore, load along with the abrasive size and sliding distance were used in this study. Temperature also affects the performance of materials hence, taken as fourth factor in this study. Thus four factors load, abrasive size, sliding distance, and temperature with three levels of each factor were used in the present study. These factors were designated as L (load, N), A (abrasive size, μm), sliding distance (S), and temperature (T), respectively. The coded value of upper, middle, and lower level of the three factors is designated by +1, 0, and −1, respectively. The actual and coded values (in parentheses) of various factors used in the present study are shown in Table 2. The experimental design matrix for different runs is shown in Table 3. The relation between the actual and coded value of a factor is given as:

$$Coded\ value = \frac{Actual\ test\ conditions - Mean\ test\ conditions}{Range\ of\ test\ conditions\ /\ 2}$$

(Eq 1)

2.3 Wear Test

Wear behavior of HVOF sprayed coatings was studied using pin on abrasive disk tester with spiral movement of the pin. Coated pins of size $5 \times 5 \times 35$ mm were held against abrasive medium made from water-proof SiC abrasive papers and mounted on a steel disk (210×20 mm), which was rotated at 200 ± 4, 296 ± 5, and 368 ± 5 rpm (revolution per minute) corresponding to the sliding distance of 25, 55, and 85 m/min. The slide carrying the wear pin was moved radially to get the spiral motion under a constant increment of 0.2 mm of the wear pin. The coated pins and disk with the abrasive papers were enclosed in a heating chamber. Three thermocouples were used for measuring the temperature of the heating chamber. The test temperature was controlled with the temperature controller unit (target temperature $\pm 5\ °C$). The tester was allowed to run idle for 2 min in order to attain the constant rpm (without reciprocating motion). Afterwards, the load was applied and simultaneously the reciprocating unit was switched on to have a spiral motion of the wear pin. Wear tests were conducted randomly according to design matrix (Table 3) with two replications of each run. Average values of abrasive wear have been reported in Table 3. An electronic balance (accuracy 0.0001 g) was used for weighing the samples before and after abrasive wear tests. Weight loss (g) was used as a measure of abrasive wear.

Fig. 1 Morphology of unmodified 1006 coating powder

Table 1 HVOF spraying parameters for unmodified 1006 and modified 1006C powder coatings

Spraying parameter	Parameter setting
Pressure—Oxygen, psi	11.7
Flow—Oxygen, L/min	32
Pressure—Hydrogen, psi	9.6
Hydrogen—Oxygen, L/min	62
Pressure—Air, psi	7.4
Flow—Air, L/min	44
Pressure—Carrier gas—Nitrogen, psi	10
Flow—Carrier gas—Nitrogen, L/min	44
Powder flow, g/min	50
Spraying distance, mm	250
Traverse speed of gun, mm/s	550
Maximum surface temperature during spraying, °C	90

Table 2 Various factors and their levels used in abrasive wear study

Factor	Lower level	Middle level	Upper level
Load, N	5 (−1)	15 (0)	25 (+1)
Abrasive size, μm {grit size}	20 ± 2* {500} (−1)	60 ± 4* {220} (0)	100 ± 5* {120} (+1)
Sliding distance, m	25 (−1)	55 (0)	85 (+1)
Temperature, °C	50 (−1)	100 (0)	150 (+1)

*As given by manufacturer

Table 3 Design matrix showing the abrasive wear test parameters (factors) with their actual and coded levels (in small braces) and abrasive wear test results unmodified 1006 and modified 1006C HVOF sprayed coatings

Run no.	Load (L), N	Abrasive size (A), μm	Sliding distance (S), m	Temperature, (T), °C	Av. wt. loss unmodified 1006 coating, g	Av. wt. loss modified 1006C coating, g
1	25 (+1)	100 (+1)	25 (−1)	150 (+1)	0.0225	0.0201
2	5 (−1)	100 (+1)	85 (+1)	50 (−1)	0.0238	0.0223
3	5 (−1)	100 (+1)	25 (−1)	150 (+1)	0.0072	0.0075
4	25 (+1)	60 (0)	55 (0)	100 (0)	0.0377	0.0362
5	25 (+1)	100 (+1)	25 (−1)	50 (−1)	0.039	0.0379
6	5 (−1)	60 (0)	55 (0)	100 (0)	0.0132	0.0116
7	25 (+1)	20 (−1)	25 (−1)	150 (+1)	0.0202	0.0189
8	5 (−1)	100 (+1)	85 (+1)	150 (+1)	0.0284	0.0257
9	25 (+1)	100 (+1)	85 (+1)	50 (−1)	0.0968	0.0859
10	15 (0)	60 (0)	85 (+1)	100 (0)	0.0523	0.0473
11	5 (−1)	20 (−1)	85 (+1)	150 (+1)	0.0153	0.0163
12	25 (+1)	100 (+1)	85 (+1)	150 (+1)	0.0801	0.0738
13	15 (0)	20 (−1)	55 (0)	100 (0)	0.0158	0.0141
14	25 (+1)	20 (−1)	25 (−1)	50 (−1)	0.0165	0.0148
15	15 (0)	60 (0)	55 (0)	100 (0)	0.0278	0.0245
16	15 (0)	60 (0)	25 (−1)	100 (0)	0.0137	0.0129
17	5 (−1)	20 (−1)	25 (−1)	50 (−1)	0.0027	0.0037
18	5 (−1)	20 (−1)	85 (+1)	50 (−1)	0.0124	0.0114
19	25 (+1)	20 (−1)	85 (+1)	50 (−1)	0.0388	0.0351
20	5 (−1)	100 (+1)	25 (−1)	50 (−1)	0.0140	0.0124
21	15 (0)	60 (0)	55 (0)	150 (+1)	0.0207	0.0184
22	15 (0)	60 (0)	55 (0)	50 (−1)	0.0302	0.0267
23	5 (0)	20 (−1)	25 (−1)	150 (+1)	0.0013	0.0018
24	25 (+1)	20 (−1)	85 (+1)	150(+1)	0.0444	0.0405
25	15 (0)	100 (+1)	55 (0)	100 (0)	0.0383	0.0349
26	15 (0)	60 (0)	55 (0)	100(0)	0.0317	0.0275

3. Results and Discussion

3.1 Microstructure of Unmodified 1006 and Modified 1006C HVOF Sprayed Coatings

The microstructures of unmodified 1006 and modified 1006C powder coatings and their EDAX analysis are shown in Fig. 2(a)-(d) and 3(a)-(d). Both the coatings mainly showed three different regions "A", "B", and "C" as indicated by the arrows in the microstructures and accordingly these have been designated as phase "A", "B", and "C", respectively. Image analysis for volume fraction of various phases in unmodified 1006 and modified 1006C modified coatings (six micrographs of each coating) was carried out by Dewinter Material Plus 4.1 software. Average values showed that the volume fraction of phase "A" was found 57.5 and 54.1% in unmodified 1006 powder coating and modified 1006C coatings, respectively. The volume fraction of phase "B" was found

to be 34.9 and 39.6% whereas that of phase "C" was found as 7.2 and 6.3% in unmodified 1006 and modified 1006C coatings, respectively. It was also noticed that the volume fraction of phase "A" and "C" was slightly reduced whereas the volume fraction of phase "B" was increased with the addition of CeO_2 in unmodified 1006 powder coating. The other details of microstructure and XRD analysis were described in detail by the author (Ref 25).

3.2 Microhardness of Unmodified 1006 and Modified 1006C HVOF Sprayed Coatings

The microhardness of unmodified 1006 and modified 1006C powder coatings as a function of distance from the coating-substrate interface and average microhardness of coatings is shown in Fig. 4. It can be noticed that the modified 1006C coating showed higher hardness than the unmodified 1006 coating. The increase of microhardness of modified 1006C coating is due to microstructure refining
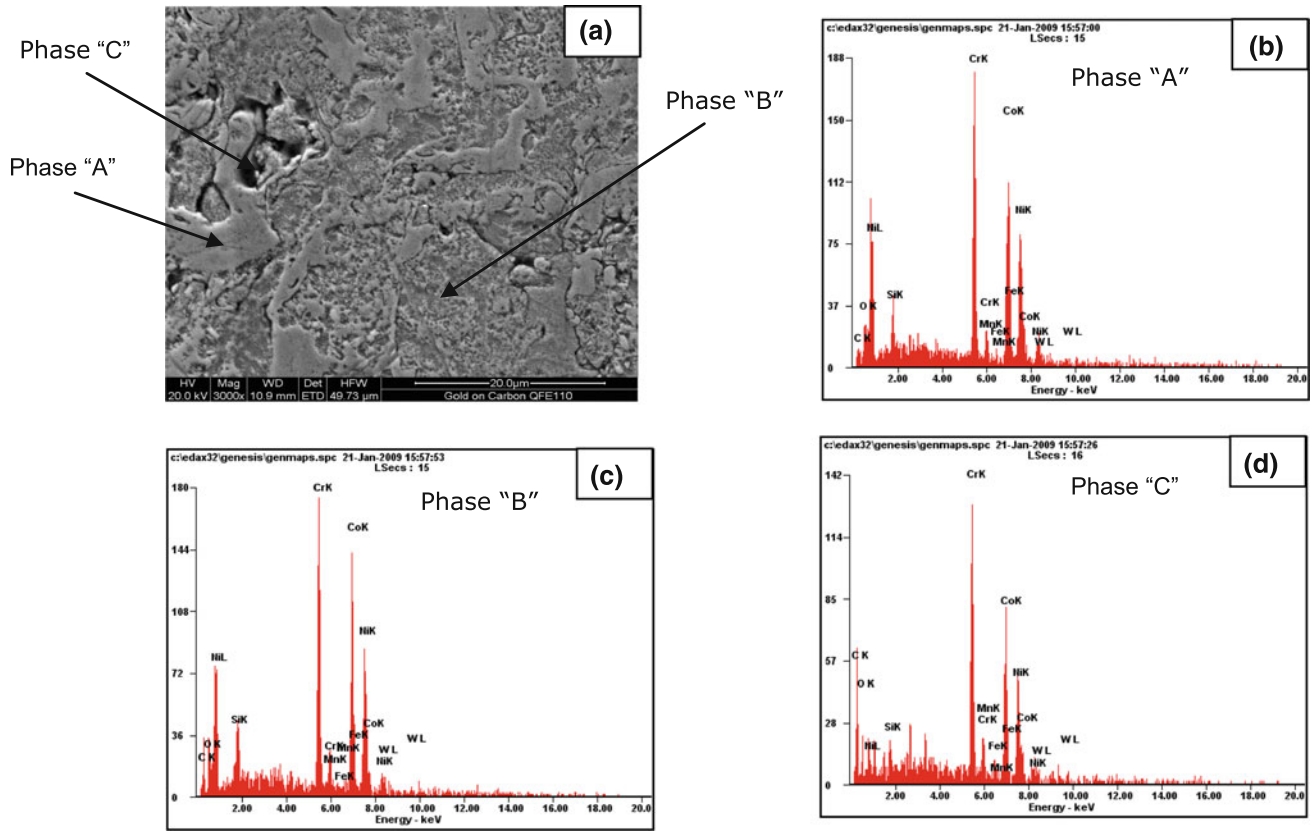
Fig. 2 Microstructure and EDAX analysis of various phases present in unmodified 1006 coating (a) BSE micrograph of microstructure and EDAX spectra of (b) phase "A", (c) phase "B", and (d) phase "C"

effect of rare earths and resulting in uniform distribution of various elements (Ref 17, 21).

3.3 Abrasive Wear Model

In the present work RSM was applied for developing the mathematical abrasive wear models in the form of multiple regression equations for the abrasive wear. In applying the RSM the dependent variable (abrasive wear) is viewed as a surface to which the model is fitted as given below:

$$AW = b_0 + \sum_{i=1}^{k} b_i x_i + \sum_{i=1}^{k} b_{ii} x_i^2 + \sum_{i=1}^{k-1} \sum_{j=i+1}^{k} b_{ij} x_i x_j + \varepsilon r$$

$$(\text{Eq } 2)$$

The other details related to RSM and ANOVA (Table 4) were described by the author in his earlier work (Ref 25). The main factors and their significant interactions are included in the final abrasive wear model while the insignificant interactions are excluded from the abrasive wear model. Load (L), abrasive size (A), and sliding distance (S) were the significant factors while load and abrasive size (LA), load and sliding distance (LS) and

abrasive size and sliding distance (AS) were the significant interactions. The abrasive wear model generated in terms of coded (Eq 3, 4) and actual factor values (Eq 5, 6), respectively, are given below:

$$AW(\text{Unmodifed } 1006_{\text{Coded}})$$
$$= 0.029 + 0.015L + 0.01A$$
$$\quad + 0.014S - 1.894 \times 10^{-3} T + 4.8 \times 10^{-3} LA + 6.7$$
$$\quad \times 10^{-3} LS + 4.763 \times 10^{-3} AS \pm \varepsilon_r \qquad (\text{Eq } 3)$$

$$AW(\text{Modified } 1006C_{\text{Coded}})$$
$$= 0.026 + 0.014L + 9.11$$
$$\quad \times 10^{-3} A + 0.013S - 1.511 \times 10^{-3} T + 4.61 \times 10^{-3} LA$$
$$\quad + 5.83 \times 10^{-3} LS + 4.11 \times 10^{-3} AS \pm \varepsilon_r \qquad (\text{Eq } 4)$$

$$AW(\text{Unmodified } 1006_{\text{actual}})$$
$$= 0.0104 - 4.056 \times 10^{-4} L$$
$$\quad - 1.445 \times 10^{-4} A - 1.005 \times 10^{-4} S - 3.789 \times 10^{-5} T$$
$$\quad + 1.2 \times 10^{-5} LA + 2.233 LS + 3.969 \times 10^{-6} AS \pm \varepsilon_r$$
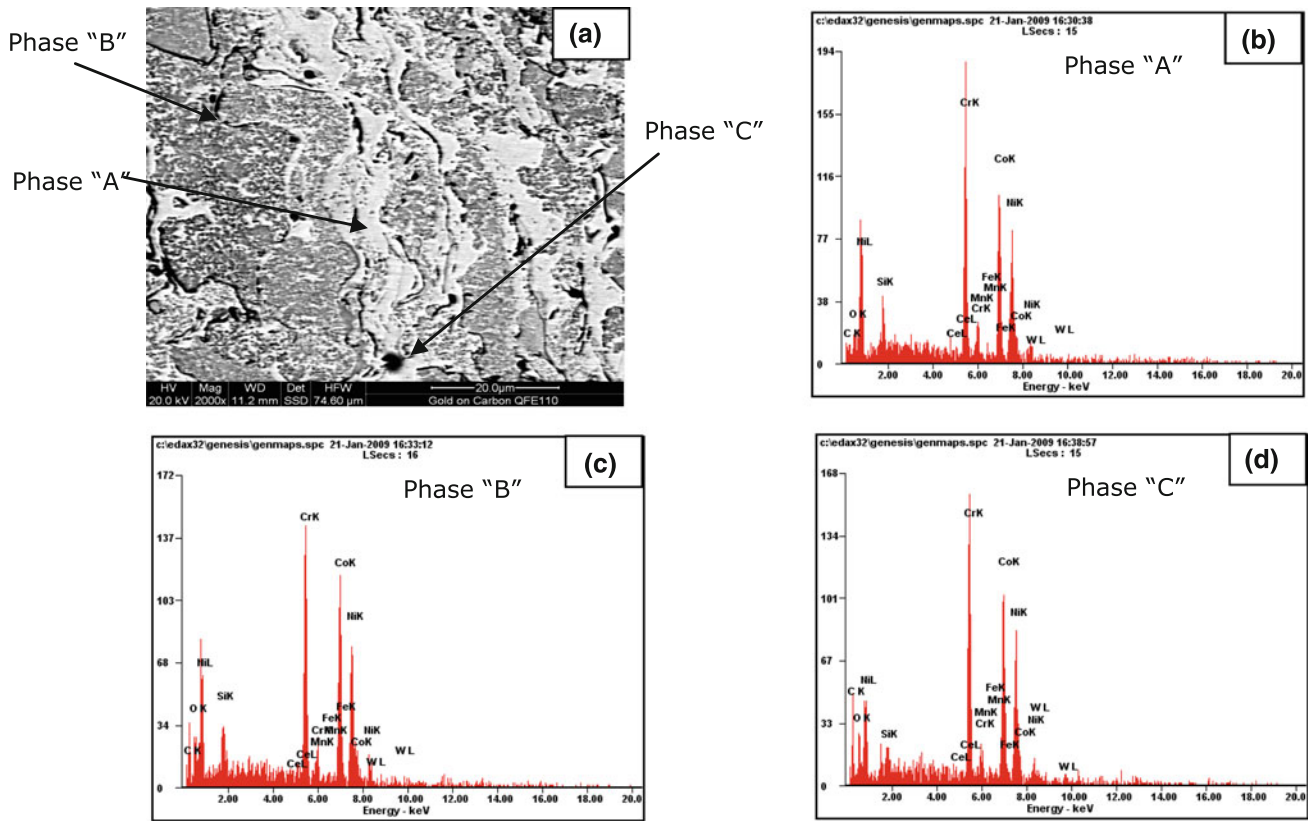
$$(\text{Eq } 5)$$

Fig. 3 Microstructure and EDAX analysis of various phases present in modified 1006C coating (a) BSE micrograph of microstructure and EDAX spectra of (b) phase "A", (c) phase "B", and (d) phase "C"
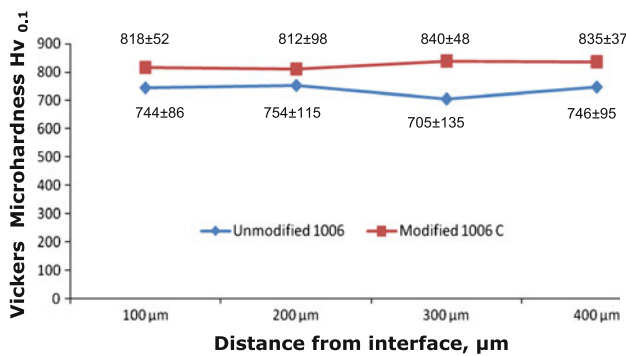

Fig. 4 Microhardness as a function of distance from coating-substrate interface of unmodified 1006 and modified 1006C HVOF sprayed coatings

AW (Modified $1006C_{actual}$)

$$= 9.17 \times 10^{-3} - 3.68 \times 10^{-4}L$$
$$- 1.33 \times 10^{-4}A - 7.41 \times 10^{-5}S - 3.02 \times 10^{-5}T + 1.15$$
$$\times 10^{-5}LA + 1.944 \times 10^{-5}LS + 3.422 \times 10^{-6}AS \pm \varepsilon_r$$

$$(Eq \ 6)$$

3.4 Validity of the Abrasive Wear Model

The validity of the abrasive wear model was evaluated by conducting abrasive wear tests on coatings at different values of the experimental factors such as applied load (L), abrasive sizes (A), sliding distance (S), and temperature (T). The actual and coded value of various factors used in confirmation tests are shown in Table 5. The variations between the experimental and the calculated values are of the order of 2-8% as shown in Table 6.

3.5 Effect of Individual Variables on Abrasive Wear

The abrasive wear response surface model in terms of coded level (+1, 0, and −1) of applied factors (L, A, S, and T) and their interactions (LA, LS, and AS) of unmodified 1006 and modified 1006C HVOF sprayed coating is shown in Eq 3 and 4 while model in terms of actual level of applied factors and their interactions is shown in Eq 5 and 6. The effects of individual factors and their combined effects on abrasive wear of modified 1006C HVOF sprayed coatings can be described by considering the Eq 4 because all the factors are at the same coded level (+1, 0, and −1). The constant 0.026 in Eq 4 indicates the overall mean abrasive wear of modified 1006C coating under all test conditions. This equation further indicates that the

Table 4 Analysis of variance (ANOVA) for abrasive wear model of modified 1006C HVOF sprayed coating

Source	Sum squares	Degrees of freedom	Mean square	*F* value	Prob $> F$	
Model	9.069×10^{-3}	7	1.296×10^{-3}	38.89	<0.0001	Significant
Load *L*	3.486×10^{-3}	1	3.486×10^{-3}	104.65	<0.0001	
Abrasive size *A*	1.429×10^{-3}	1	1.429×10^{-3}	44.80	<0.0001	
Sliding distance *S*	2.896×10^{-3}	1	2.896×10^{-3}	86.93	<0.0001	
Temp. *T*	4.11×10^{-5}	1	4.11×10^{-5}	1.23	28.13	
Interaction *LA*	3.395×10^{-4}	1	3.395×10^{-4}	10.19	0.0050	
Interaction *LS*	5.441×10^{-4}	1	5.441×10^{-4}	16.33	0.0008	
Interaction *AS*	2.698×10^{-4}	1	2.698×10^{-4}	8.10	0.0107	
Residual error	5.996×10^{-4}	18	3.331×10^{-5}			
Lack of fit	5.951×10^{-4}	17	3.501×10^{-5}	7.78	0.2755	Not significant
Pure error	4.5×10^{-6}	1	4.5×10^{-6}			

Table 5 Abrasive wear test parameters and their levels (in actual and coded form) used for conducting the confirmation tests to validate the abrasive wear models for unmodified 1006 and modified 1006C coatings

Confirmation run no.	Load (*L*), N	Abrasive size (*A*), μm	Sliding distance (*S*), m	Temperature (*T*), °C
1	10 (−0.5)	80 ± 3 (+0.5)	70 (+0.5)	100 (0)
2	20 (+0.5)	42 ± 2 (-0.45)	70 (+0.5)	100 (0)

Table 6 Abrasive wear test results obtained from modeled equations and experimental confirmation abrasive wear tests of unmodified 1006 and modified 1006C HVOF sprayed coatings

	Confirmation run no. 1			Confirmation run no. 2		
HVOF coatings	Modeled abrasive wear, g	Experimental abrasive wear, g	Error, %	Modeled abrasive wear, g	Experimental abrasive wear, g	Error, %
Unmodified 1006	0.0314	0.0302	3.8	0.0384	0.0408	5.9
Modified 1006C	0.0286	0.0311	8.03	0.0349	0.0356	1.96

coefficient associated with load (*L*), abrasive size (*A*), sliding distance (*S*), and temperature (*T*) are 0.014, 9.11×10^{-3}, 0.013, and 1.511×10^{-3}, respectively. The value of the constant associated with each factor shows the extent of damage caused by that factor in abrasive wear of the coatings (Ref 25, 26).

The effect of load, abrasive size, sliding distance, and temperature on abrasive wear is shown graphically in Fig. 5(a)-(d) and 6(a)-(c). The abrasive wear increases with the increase in load as shown in Fig. 5(a). The increase in abrasive wear is due to the fact that the load determines the depth and width of penetration of abrasive particles in the coating material. With the increase in load, the depth and width of penetration of abrasive particles increases as shown in Fig. 7(a)-(d). This in turn increases the volume of material removed from the coating, hence, increasing the abrasive wear. This is in agreement with the published literature (Ref 28-33).

Figure 5(b) shows the increase in abrasive wear with the increase of abrasive size. As the abrasive size increases, the actual contact area increases due to which the effective load on abrasive particles increases (Ref 26). An increase in effective load leads to deeper and wider grooves as discussed above, which in turn cause more

abrasive wear of the coating. While in the case of small abrasive size particles, the width and depth of penetration is reduced due to the lower height of projection of fine size abrasive particles, which results in reduced wear of coatings (Fig. 5b) (Ref 26). These facts are in agreement with the earlier findings of various researchers (Ref 30, 34-38). The low abrasive wear against fine abrasive size particles is generally attributed to rapid clogging of the fine abrasive particles (Ref 30).

The increase in sliding distance also increases the abrasive wear as shown in Fig. 5(c). There is a prolonged interaction of abrasive particles with the coating material at higher sliding distances, resulting in removal of large volume of material and hence, the increased abrasive wear (Ref 28, 29). The negative sign associated with the temperature term (Eq 4), indicates a reduction in abrasive wear with the increase in temperature. The reduction in abrasive wear with increase in temperature (Fig. 5d) may be due to removal of some abrasive particles from the abrasive paper at high temperature, which results in three-body abrasive wear. The weight loss in three-body abrasive wear is lower than two-body abrasive wear (Ref 39). Moreover, SEM study of worn surfaces also confirms the removal of abrasive particles at high temperature (Fig. 7d).
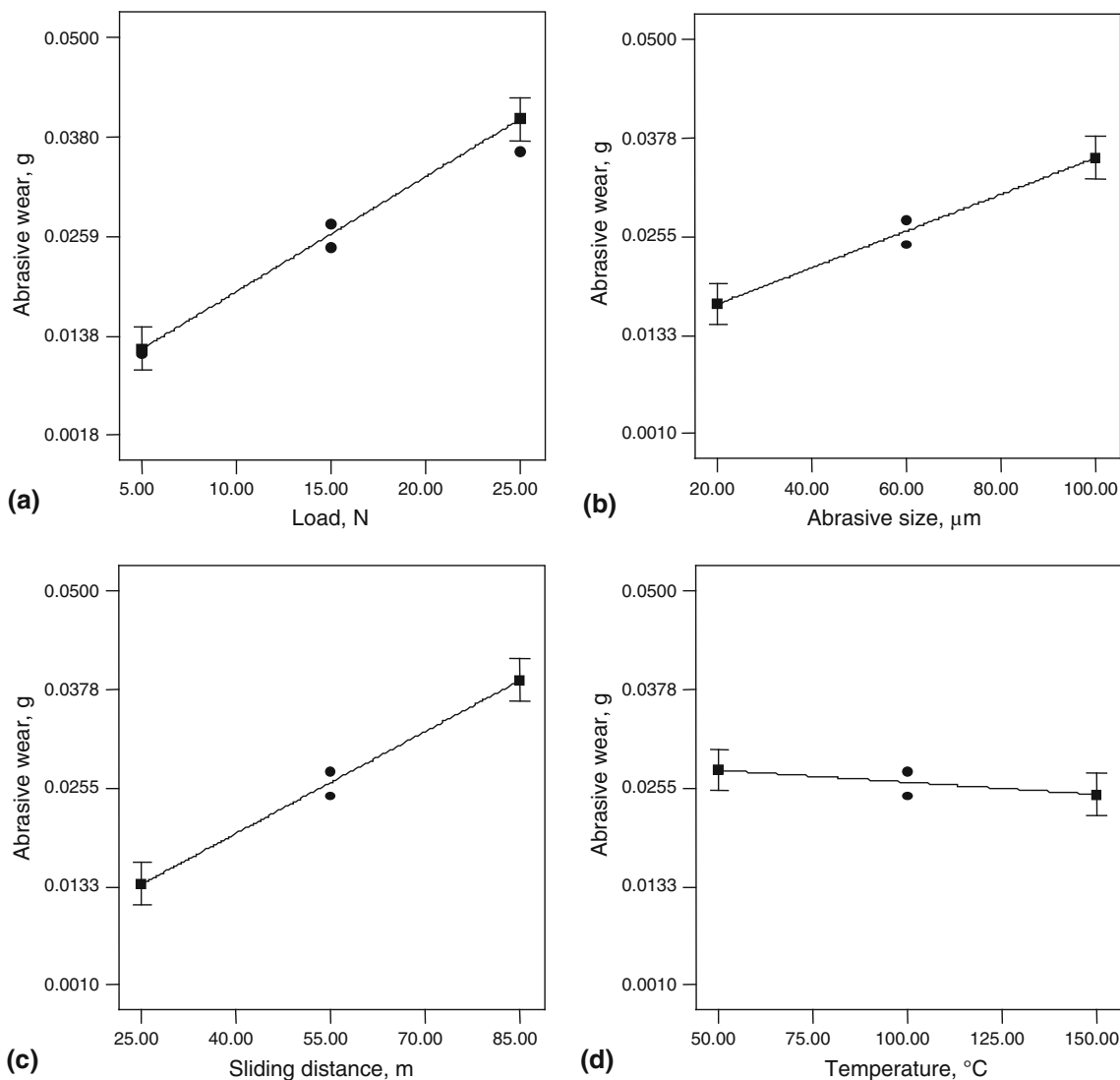
Fig. 5 Single factor (a) load (L), (b) abrasive size (A), (c) sliding distance (S), and (d) temperature (T) effect on abrasive wear of modified 1006C coating

3.6 Combined Effects Between Applied Factors on Abrasive Wear of Unmodified 1006 and Modified 1006C HVOF Sprayed Coating

The coefficients associated with the interaction terms load-abrasive size (LA), load-sliding distance (LS), and abrasives size-sliding distance (AS) are 4.61×10^{-3}, 5.83×10^{-3}, and 4.11×10^{-3}, respectively, in the response surface model (Eq 4) of modified 1006C powder coating. These coefficients indicate the extent of damage caused by combined effect between different factors on abrasive wear (Ref 25, 26). Among the various combined effects of applied factors on abrasive wear of modified 1006C coating, load-sliding distance (LS) interaction effect is greater than the other two interactions namely load-abrasives size (LA), and abrasives size-sliding distance (AS). The abrasives size-sliding distance (AS) interaction effect is the lowest among the three significant interactions. The

combined effects of various factors on abrasive wear of modified 1006C HVOF sprayed coating are shown in Fig. 6(a)-(c).

The interaction effects between load-abrasives size (LA) on abrasive wear (Fig. 6a) of modified 1006C powder coating shows that the abrasive wear of coatings increases with increase in both load and abrasives size. Moreover, the effect of increase in load on abrasive wear against large abrasives is more predominant than against fine abrasives (Fig. 6a) and the same is attributed to the fact that the load determines the depth of penetration while abrasive size determines the width of wear groove in the coating. Thus, with the increase in both load and abrasives size, the depth and width of wear grooves increases, which in turn cause increased volume of material removed and hence the increase in abrasive wear of the coating. The opposite is also true in the case of low load and small abrasives size particles,
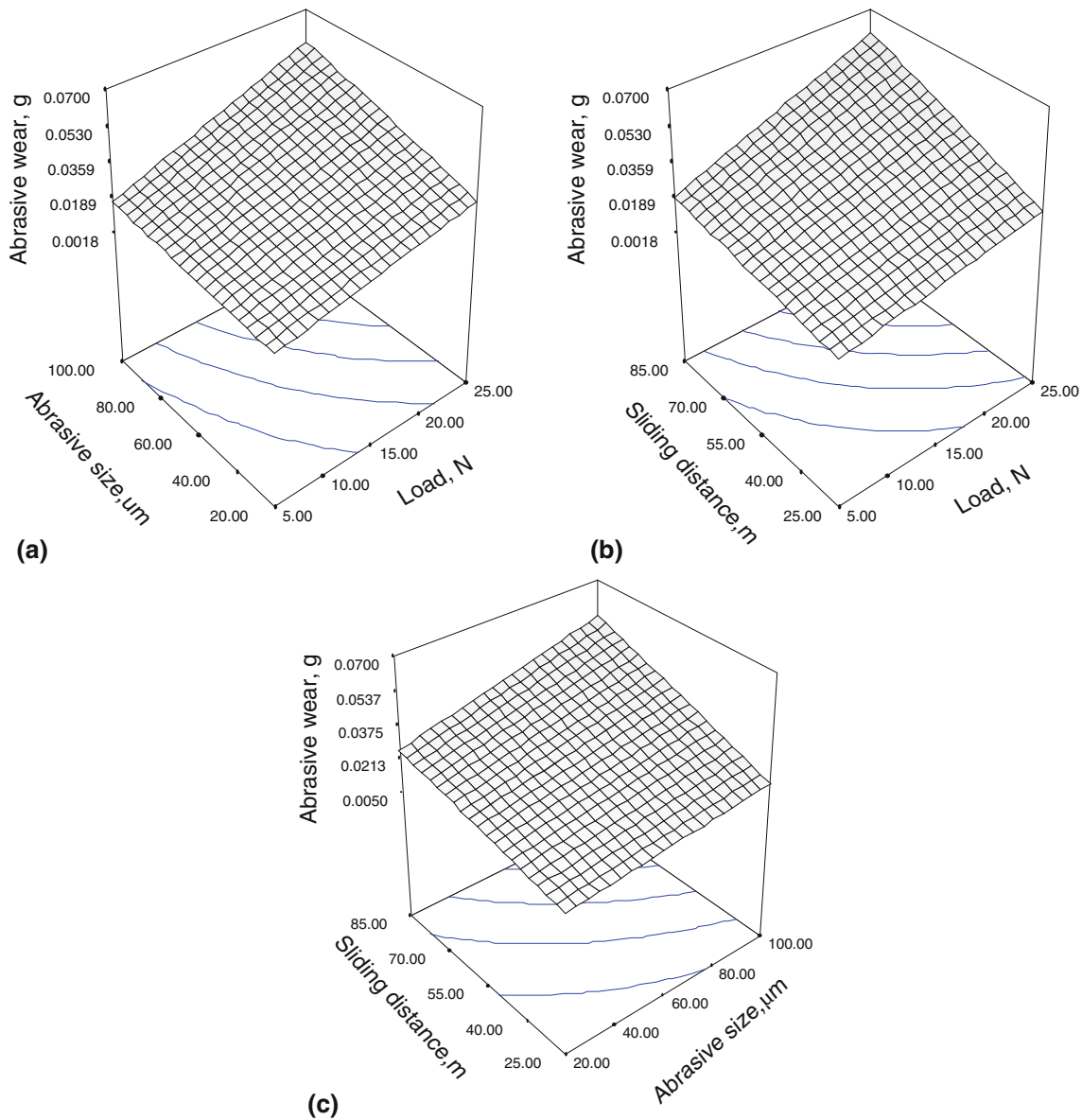
Fig. 6 3 D surface plots showing the relationship between abrasive wear and interaction effects between (a) load-abrasive size (*LA*), (b) load-sliding distance (*LS*), and (c) abrasive size-sliding distance (*AS*) of modified 1006C powder coating

thus leading to low abrasive wear of the coating at low load-abrasives size interaction.

The combined effect between load and sliding distance (*LS*) on abrasive wear of modified 1006C coating is shown graphically in Fig. 6(b). It is again concluded from Fig. 6(b) that the wear of coating increases with increase in both the load and sliding distance. The effect of increase in load on abrasive wear is more predominant than the increase in sliding distance. This is due to the fact that the load determines the width and depth of penetration of abrasive particles in the coating while sliding distance determines the length of wear groove. The increase in load and sliding distance increase the depth, width, and length of abrasive groove which in turn increases the volume of material removed and consequently the increase in

abrasive wear of the coating. Therefore, higher abrasive wear is observed at higher load-sliding distance interaction as compared to that for low load-sliding distance interaction (Ref 28-31).

The interaction effect between abrasives size and sliding distance (*AS*) on abrasive wear of modified 1006C powder coating (Fig. 6c) shows that the wear of coating increases with the increase in both sliding distance and abrasives size. Again the effect of increase in sliding distance on abrasive wear is more predominant than that of abrasives size. It can be observed from 3D graphs that the effect of increase in sliding distance on wear of coatings is more against large abrasives as compared to fine abrasive particles. This due to the fact that with the increase in abrasives size, effective load on abrasives increases which
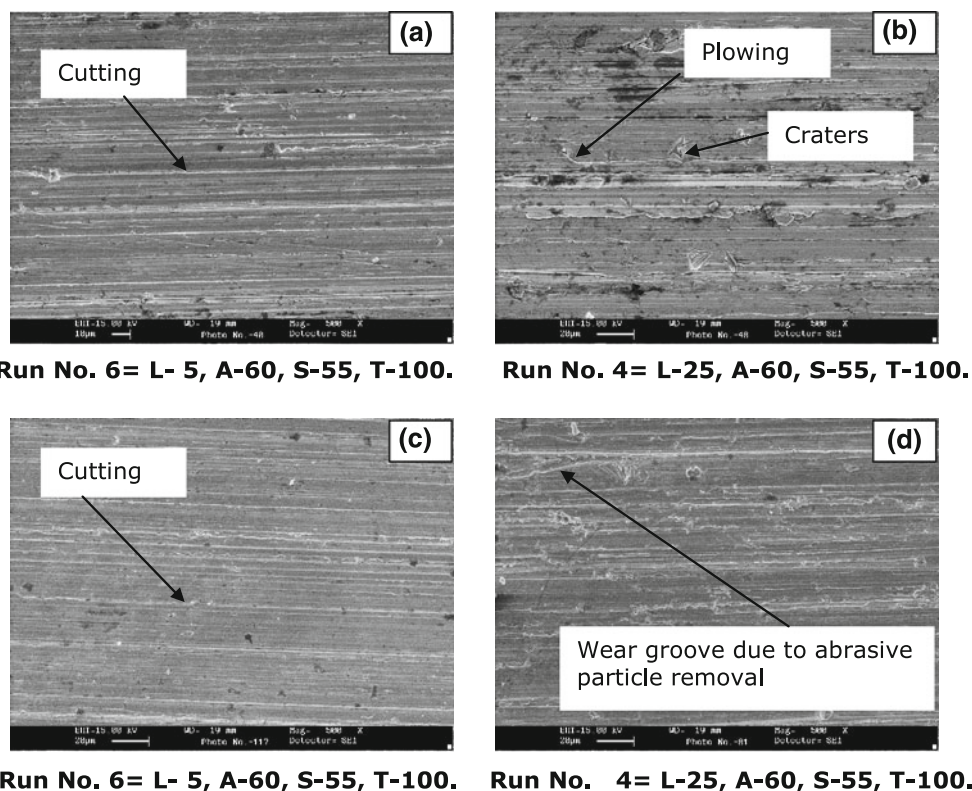
Fig. 7 SEM micrographs of worn surfaces of (a, b) unmodified 1006 and (c, d) modified 1006C HVOF sprayed coatings

results in deeper and wider wear grooves as compared to fine abrasives sizes (Ref 30, 34-38), while sliding distance determines the length of wear groove and which in turn increases abrasive wear. The single factor and interaction effects for unmodified 1006 coating can be explained on the similar lines as described above.

3.7 SEM Study of Worn Surfaces of Unmodified 1006 and Modified 1006C HVOF Sprayed Coatings

SEM analysis of the worn surfaces of unmodified 1006 and modified 1006C HVOF sprayed coatings are shown in Fig. 7(a)-(d). Cutting was observed as the material removal mechanism in these coatings (Fig. 7a-d). The extent of damage by cutting mechanism is lower in modified 1006C coating (Fig. 7c, d) as compared to unmodified 1006 coating (Fig. 7a, b). This is due to higher hardness of the modified 1006C coating. The width and depth of penetration of abrasives decreases with the increase in hardness, which results in finer wear grooves in the coating. It means lower volume of material is removed and hence, results in lower abrasive wear of the coating (Ref 26). The reduction in abrasive wear with increase in temperature (Fig. 5d) may be due to removal of some abrasive particles from the abrasive paper at high temperature, which results in three-body abrasive wear. The weight loss in three-body abrasive wear is lower than two-body abrasive wear (Ref 39). Moreover, SEM study of worn surfaces also confirms the removal of abrasive particles at high temperature (Fig. 7d).

4. Conclusions

The following conclusions can be drawn from the present study:

1. RSM can be used to develop a statistical model for the prediction and understanding of wear behavior of coatings in terms of individual factors (L, A, S, and T) as well as in terms of the combined effects (LA, LS, and AS) of various factors.

2. The load, abrasive size, and sliding distance has a more severe effect on abrasive wear of the coating as compared to temperature.

3. Interactions effects of various factors on abrasive wear are one order less than their main factor effects. The interaction effect of abrasive size and sliding distance (AS) is considerably higher than load and abrasive size (LA).

4. The abrasive wear of modified 1006C coating is lower than unmodified 1006 coating.

5. Cutting was the main wear mechanism found in unmodified 1006 and modified 1006C coatings but the extent of cutting is low in modified 1006C coating as compared to unmodified 1006 coating.

References

1. H. Hamatani, Y. Ichiyama, and J. Kobayashi, Mechanical and Thermal Properties of HVOF Sprayed Ni Based Alloys with Carbide, *Sci. Technol. Adv. Mater.*, 2002, **3**, p 319-326

2. T. Burakowski and T. Wieszchon, *Surface Engineering of Metals: Principle, Equipments and Technology*, CRC Press, Boca Raton, 1998

3. K. Hajmrle, P. Fiala, A.P. Chilkowich, L. Shiembob, C. Moreau, and B. Marple, "ITSC 2003," Orlando, ASM International, Materials Park, OH, USA, 2003, p 735

4. M.Z. Yi, J.W. He, B.Y. Huang, and H. Zhou, Friction and Wear Behaviour and Abradability of Abradable Seal Coating, *Wear*, 1999, **231**, p 47-53

5. T. Sudaprasert, P.H. Shipway, and D.G. McCartney, Sliding Wear Behaviour of HVOF Sprayed WC-Co Coatings Deposited with Both Gas-Fuelled and Liquid-Fuelled Systems, *Wear*, 2003, **255**, p 943-949

6. D.A. Stewart, P.H. Shipway, and D.G. McCartney, Abrasive Wear Behaviour of Conventional and Nano-composite HVOF-Sprayed W-Co Coatings, *Wear*, 1999, **225-229**, p 789-798

7. C. Monticelli, A. Frignani, and F. Zucchi, Investigation on the Corrosion Process of Carbon Steel Coated by HVOF WC/Co Cermets in Neutral Solution, *Corros. Sci.*, 2004, **46**, p 1225-1237

8. D.W. Wheeler and R.J.K. Wood, Erosion of Hard Surface Coatings for Use in Offshore Gate Valves, *Wear*, 2005, **258**, p 526-536

9. B.S. Mann and V. Arya, HVOF Coating and Surface Treatment for Enhancing Droplet Erosion Resistance of Steam Turbine Blades, *Wear*, 2003, **254**, p 652-667

10. B.Q. Wang and Z.R. Shui, Hot Erosion Behavior of Carbide-Metal Composite Coatings, *J. Mater. Process. Technol.*, 2003, **143-144**, p 87-92

11. S. Harsha, D.K. Dwivedi, and A. Agrawal, Influence of WC Addition in Co-Cr-W-Ni-C Flame Sprayed Coatings on Microstructure, Microhardness and Wear Behavior, *Surf. Coat. Technol.*, 2007, **201**, p 5766-5775

12. N. Minoru, Effect of $TiC-Cr_3C_2$ Particles Content on Abrasive Wear Resistance of Co-Base Overlay Weld Alloy, *J. Jpn. Weld. Soc.*, 1993, **11**, p 156-161

13. A.K. Maiti, N. Mukhopadhyay, and R. Raman, Effect of Adding WC Powder to the Feedstock of WC-Co-Cr Based HVOF Coating and Its Impact on Erosion and Abrasion Resistance, *Surf. Coat. Technol.*, 2007, **201**, p 7781-7788

14. K.L. Wang, Q.B. Zhang, M.L. Sun, X.G. Wei, and Y.M. Zhu, Microstructure and Corrosion Resistance of Laser Clad Coatings with Rare Earth Elements, *Corros. Sci.*, 2001, **43**, p 255-267

15. X.H. Wang, M. Zhang, Z.D. Zhou, and S.Y. Qu, Microstructure and Properties of Laser Clad TiC + NiCrBSi + Rare Earth Composite Coatings, *Surf. Coat. Technol.*, 2002, **161**, p 195-199

16. G.M. Zhao and K.L. Wang, Effect of La_2O_3 on Corrosion Resistance of Laser Clad Ferrite-Based Alloy Coatings, *Corros. Sci.*, 2006, **48**, p 273-284

17. Z.Z. Zhang, Z.P. Wang, and B.N. Liang, Effect of CeO_2 on Microstructure and Bond Strength of Fe-Ni-Cr Alloy, *J. Rare Earth*, 2005, **23**, p 73-76

18. Z.Y. Zhang, H.Q. Li, and H.X. Zhou, *Rare Met. Mater. Eng.*, 2005, **34**(Suppl. 2), p 384-387

19. Z.Y. Zhang, H.Q. Li, and J. Zhang, *J. Rare Earth*, 2004, **22**, p 180-184 (Special Issue)

20. X.Y. Cheng, X.B. Xie, and S. Jiang, Influence of Lanthanum on Tribological Properties and Microstructure of Laser Clad B + Fe + Si Composite Coatings, *J. Rare Earth*, 2004, **22**, p 687-690

21. S. Sharma, D.K. Dwivedi, and P.K. Jain, Effect of CeO_2 Addition on the Microstructure, Hardness, and Abrasive Wear Behavior of Flame-Sprayed Ni-Based Coatings, *Proc. Inst. Mech. Eng. Part J*, 2008, **222**, p 925-933

22. S. Sharma, D.K. Dwivedi, and P.K. Jain, Effect of La_2O_3 Addition on the Microstructure, Hardness and Abrasive Wear Behavior of Flame Sprayed Ni Based Coatings, *Wear*, 2009, **267**, p 853-859

23. M. Li, S. Zhang, H. Li, Y. He, J.-H. Yoon, and T.-Y. Cho, Effect of Nano-CeO_2 on Cobalt-Based Alloy Laser Coatings, *J. Mater. Process. Technol.*, 2008, **202**, p 107-111

24. Z. Zhang, X. Lu, B. Han, and J. Luo, Rare Earth Effect on Microstructure, Mechanical and Tribological Properties of CoCrW Coatings, *Mater. Sci. Eng., A*, 2007, **444**, p 92-98

25. S. Sharma, Erosive Wear Study of Rare Earth Modified HVOF Sprayed Coatings Using Design of Experiment, *J. Therm. Spray Technol.*, 2012, **21**, p 49-62

26. K. Venkateswarlu, S. Mohapatra, R.G. Rao, A.K. Ray, L.C. Pathak, and D.P. Mondal, High Abrasive Wear Response of Diamond Reinforced Composite Coating: A Factorial Design Approach, *Tribol. Lett.*, 2006, **24**, p 7-14

27. E.D. Rabinowicz, *Friction and Wear of Work Hardening in the Design of Wear Resistant Materials*, Wiley, New York, 1965, p 168

28. M.A. Moore, A Review of Two-Body Abrasive Wear, *Wear*, 1974, **27**, p 1-17

29. E.D. Rabinowicz, *Friction and Wear of Materials*, 2nd ed., John Wiley and Sons, New York, 1995, p 193

30. B.W.E. Avient, J. Goddard, and H. Wilman, An Experimental Study of Friction and Wear During Abrasion of Metals, *Proc. R. Soc. Lond. Ser. A*, 1960, **258**, p 159-180

31. G.K. Nathan and W.J.D. Jones, The Empirical Relationship Between Abrasive Wear and the Applied Conditions, *Wear*, 1966, **9**, p 300-309

32. S. Harsha, D.K. Dwivedi, and A. Agarwal, Influence of CrC Addition in Ni-Cr-Si-B Flame Sprayed Coatings on Microstructure, Microhardness and Wear Behavior, *Int. J. Adv. Manuf. Technol.*, 2008, **38**, p 93-101

33. S. Harsha, D.K. Dwivedi, and A. Agarwal, Microstructure, Hardness and Abrasive Wear Behavior of Flame Sprayed Co-Based Alloy Coating, *Surf. Eng.*, 2007, **23**, p 1-6

34. E.D. Rabinowicz, I.A. Dunn, and P.G. Russell, A Study of Abrasive Wear Under Three-Body Condition, *Wear*, 1961, **4**, p 345-355

35. B.J. Larsen, Influence of Grit Size on Groove Formation During Sliding Abrasion, *Wear*, 1968, **11**, p 213-222

36. T.O. Mulhearn and L.E. Samuels, The Abrasion of Metals: A Model of the Process, *Wear*, 1962, **5**, p 478-498

37. S.W. Date and S. Malkin, Effects of Grit Size on Abrasion with Coated Abrasives, *Wear*, 1976, **40**, p 223-235

38. M.M. Khruschov and M.A. Babichev, *Investigation of the Wear of Metals (in Russian)*, Akademiya Nauk SSSR, Moscow, 1960, p 108-110

39. B. Bhushan, *Introduction to Tribological*, John Wiley & Sons, Inc., New York, 2002